Dimerization of *oskar* 3′ UTRs promotes hitchhiking for RNA localization in the *Drosophila* oocyte

HELENA JAMBOR,[1,3] CHRISTINE BRUNEL,[2,4] and ANNE EPHRUSSI[1,5]

[1]European Molecular Biology Laboratory, 69117 Heidelberg, Germany
[2]Architecture et Réactivité de l'ARN, Université de Strasbourg, CNRS, IBMC, 67084 Strasbourg Cedex, France

ABSTRACT

mRNA localization coupled with translational control is a highly conserved and widespread mechanism for restricting protein expression to specific sites within eukaryotic cells. In *Drosophila*, patterning of the embryo requires *oskar* mRNA transport to the posterior pole of the oocyte and translational repression prior to localization. *oskar* RNA splicing and the 3′ untranslated region (UTR) are required for posterior enrichment of the mRNA. However, reporter RNAs harboring the *oskar* 3′ UTR can localize by hitchhiking with endogenous *oskar* transcripts. Here we show that the *oskar* 3′ UTR contains a stem–loop structure that promotes RNA dimerization in vitro and hitchhiking in vivo. Mutations in the loop that abolish in vitro dimerization interfere with reporter RNA localization, and restoring loop complementarity restores hitchhiking. Our analysis provides insight into the molecular basis of RNA hitchhiking, whereby localization-incompetent RNA molecules can become locally enriched in the cytoplasm, by virtue of their association with transport-competent RNAs.

Keywords: RNA dimerization; kissing-loop interaction; *oskar* mRNA localization; RNA hitchhiking; *oskar* RNA; *Drosophila* oocyte

INTRODUCTION

In *Drosophila*, *oskar* (*osk*) mRNA is transcribed in the nurse cells of the syncytial egg chamber and transported into the developing oocyte, where it is enriched at the posterior pole (Ephrussi et al. 1991; Kim-Ha et al. 1991). *osk* translation is repressed during mRNA transport and activated once the mRNA reaches the posterior pole (Kim-Ha et al. 1995). Spatial restriction of *osk* expression is critical for proper embryonic patterning: Embryos lacking Osk protein develop no abdomen or germline, whereas embryos expressing ectopic Osk develop posterior structures in the place of the head (Lehmann and Nusslein-Volhard 1986; Ephrussi et al. 1991; Ephrussi and Lehmann 1992; Smith et al. 1992).

The signals mediating mRNA localization often reside in the 3′ untranslated region (3′ UTR) (Martin and Ephrussi 2009), and it was initially thought that the *osk* 3′ UTR contains all the *cis*-regulatory signals for posterior localization (Kim-Ha et al. 1993). However, further analysis revealed that, in addition to the 3′ UTR, splicing of the first intron is required for *osk* mRNA posterior enrichment (Hachet and Ephrussi 2004). Furthermore, localization of intronless *lacZ-osk* 3′-UTR reporter RNA was shown to depend on the presence of localized *osk* mRNA. It was therefore proposed that intronless *osk* 3′-UTR-containing messages might coassemble via their 3′ UTRs for posterior transport by hitchhiking with endogenous, transport-competent *osk* transcripts (Hachet and Ephrussi 2004).

osk mRNA was shown biochemically to be part of heavy particles containing RNA and protein (Wilhelm et al. 2003; Chekulaeva et al. 2006), and injected *osk* is transported in granules containing more than 100 molecules (Glotzer et al. 1997). Thus, hitchhiking might involve copackaging of *osk* RNA molecules into higher-order structures similar to the granules containing localized RNAs in other cell types (Martin and Ephrussi 2009).

osk hitchhiking could involve direct base-pairing between 3′ UTRs or their indirect association via an intermediate (Kim-Ha et al. 1993; Hachet and Ephrussi 2004; Jenny et al. 2006). Indeed, Bruno and PTB proteins have been shown to induce *osk* RNA oligomerization (Chekulaeva et al. 2006;

[3]**Present address:** Max Planck Institute of Molecular Cell Biology and Genetics, 01307 Dresden, Germany.
[4]**Present address:** Service du Partenariat et de la Valorisation du CNRS–Délégation Alsace, 67037 Strasbourg Cedex2, France.
[5]**Corresponding author.**
E-mail ephrussi@embl.de.
Article published online ahead of print. Article and publication date are at http://www.rnajournal.org/cgi/doi/10.1261/rna.2686411.

Besse et al. 2009). In contrast, direct base-pairing of *osk* mRNAs has not been reported. However, dimerization of RNA molecules is associated with the packaging of genomic retroviral RNA in the virion (Kung et al. 1975; Fu et al. 1994), and, in *Drosophila*, *bicoid* mRNA dimerizes in vitro and assembles into particles upon injection into embryos (Ferrandon et al. 1997; Wagner et al. 2001).

Here we demonstrate that a stem–loop in the *osk* 3′ UTR is a dimerization domain and that nucleotides promoting RNA dimerization in vitro also promote *osk* 3′-UTR-mediated hitchhiking in vivo. Our work reveals a role of RNA–RNA interaction for coordinated transport of RNA molecules within the oocyte.

RESULTS AND DISCUSSION

oskar RNA dimerizes in vitro

To investigate if *osk* 3′-UTR-mediated hitchhiking might involve direct RNA–RNA interaction, we first assessed if *osk* 3′-UTR RNA molecules (Fig. 1A) can associate in vitro, by evaluating their mobility on nondenaturing agarose gels. In vitro transcribed full-length *osk* 3′-UTR RNA runs as a single fast-migrating band under low-salt (buffer M) conditions that hinder RNA dimerization (Marquet et al. 1991; Ferrandon et al. 1997), whereas a band of slower mobility was detected under high-salt (buffer D) conditions (Fig. 1A,B, lanes 1,2). A salt-sensitive shift was also observed with the 3′ half of the *osk* 3′ UTR (Fig. 1B, lanes 5,6). Furthermore, a band of

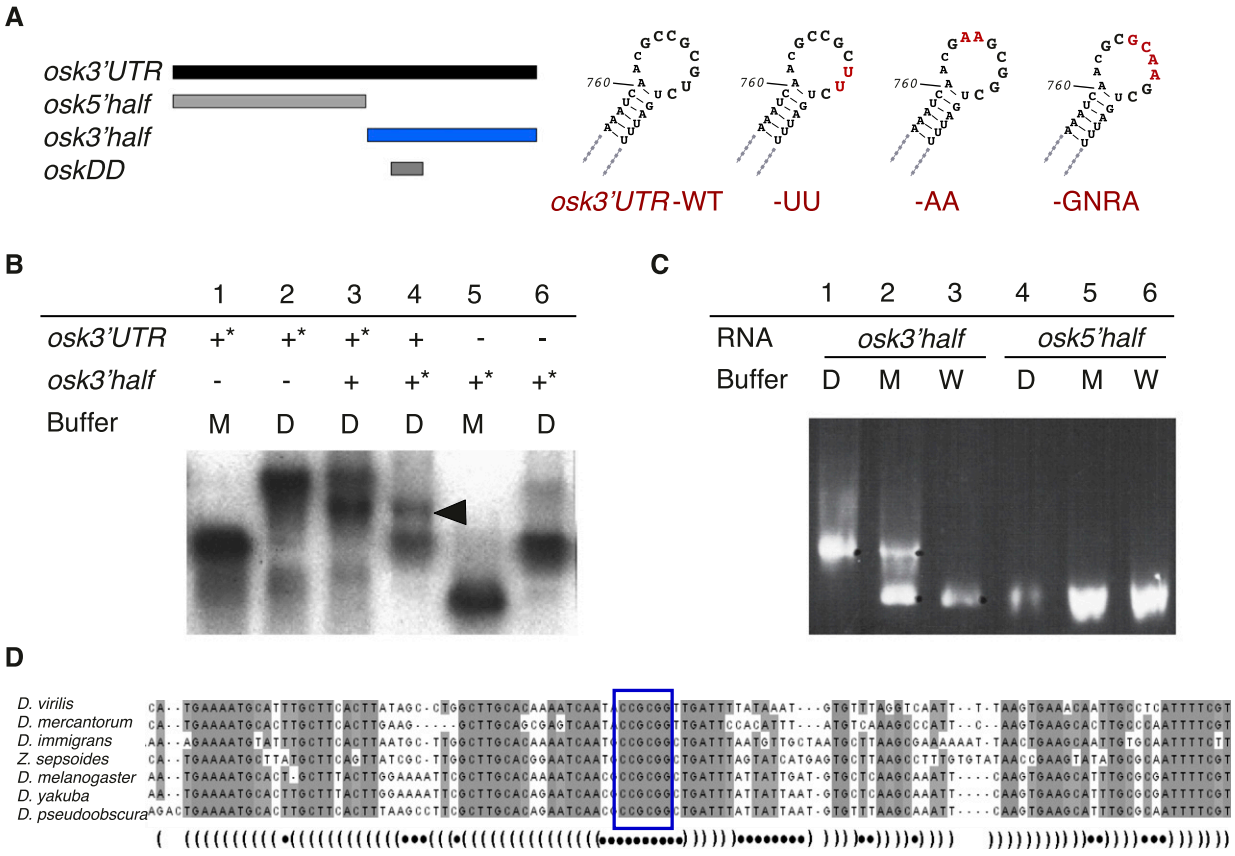

FIGURE 1. *osk* RNAs associate in vitro via a conserved region in the 3′ UTR. (*A*) Schematic representation of *osk* 3′-UTR variants analyzed in this study. (*B*) Full-length and 3′ half *osk* 3′-UTR RNAs incubated in low- (M, monomer) or high-salt (D, dimer) buffers were separated by nondenaturing gel electrophoresis. A mobility shift occurs for both *osk* 3′-UTR and 3′ half RNAs in buffer D (lanes *2*,*6*). A mobility shift of intermediate size (arrowhead) is observed when full-length and 3′ half RNAs were mixed in buffer D (lanes *3*,*4*). Radioactive-labeled RNAs are indicated by a star (*) for each lane. (*C*) 5′ half and 3′ half of *osk* 3′-UTR RNAs incubated in water, low- (M) or high-salt (D) buffers were separated by nondenaturing gel electrophoresis and stained with ethidium bromide. In water the RNAs run as a single band of low mobility (lanes *3*,*6*). The mobility of the 5′ half of *osk* 3′ UTR is identical in buffers D and M (lanes *4*,*5*). In contrast, the 3′ half RNA migrates as a band of slower mobility at the higher salt concentration (buffer D, lane *1*) than in low salt (buffer M, lane *2*). (*D*) Alignment of *oskar* 3′-UTR cDNA sequences from *Drosophila melanogaster*, *Drosophila yakuba*, *Drosophila pseudoobscura*, *Drosophila virilis*, *Drosophila immigrans*, *Drosophila mercantorum*, and *Zaprionus sepsoides*, showing a central region of high conservation among *Drosophilidae* species (nucleotides 714–827 of the *D. melanogaster osk* 3′ UTR). Highlighted in gray are regions of >75% similarity. The predicted secondary structure of the *D. melanogaster osk* is depicted *below*: (a parenthesis) a base-paired nucleotide; (a dot) a single-stranded nucleotide; (blue rectangle) the palindromic sequence within the terminal loop.

intermediate mobility appeared upon coincubation of the full-length with the 3′ half of the *osk* 3′ UTR, independent of which of the two RNAs was labeled (Fig. 1B, lanes 3,4). To address whether this salt-sensitive shift truly reflects a property of the 3′ half of the *osk* 3′ UTR to oligomerize, we next incubated the 5′ half and 3′ half RNAs in water, buffer M, and buffer D (Fig. 1A,C). The 5′ half did not form oligomers in either water or in buffers of increasing salt concentration (Fig. 1C, lanes 4–6). In contrast, the 3′ half RNA, which in water ran as a single band, appeared as a band of slower mobility in buffer M and fully shifted to the slower migrating band in buffer D (Fig. 1C, lanes 1–3). Taken together, these results show that *osk* RNA dimerizes in vitro, via sequences present in the 3′ portion of the 3′ UTR.

Several *osk* orthologs have been identified and their RNAs shown to be localized (Webster et al. 1994; data not shown). Alignment of these sequences revealed a conserved region (nucleotides 714–827) predicted to form a stem–loop within the dimerizing fragment (Fig. 1D). Interestingly, the terminal loop consists of a conserved GC-rich palindromic sequence (rectangle in Fig. 1D), a motif previously shown to mediate direct RNA–RNA interaction between *HIV-1* RNA molecules (Brunel et al. 2002). Differences between the primary sequence of the orthologs in the stem–loop either lie in predicted bulges or correspond to covarying nucleotides in the helices that should maintain the secondary structure (Fig. 1D).

To validate the predicted structure, we probed RNA molecules consisting of the 3′ half of the *osk* 3′ UTR with DMS and RNases T1 and T2. The data are summarized in Figure 2A. Under limiting conditions, RNase T1 cleaves unpaired (or single-stranded) guanines (Fig. 2A,B), while RNase T2 cleaves unpaired nucleotides with a preference for adenines (Fig. 2A). Dimethyl-sulfate (DMS) methylates Watson-Crick positions of residues located in single-stranded segments; adenines (N1-A) and cytosines (N3-C) (Fig. 2A). As illustrated in Figure 2A, the region of the *osk* 3′ UTR extending from nucleotides 714 to 827, *oskDD*, forms a stem–loop structure that is highly conserved among *Drosophilidae* species (Fig. 1D).

Comparison of RNase T1 digestion performed in either buffer M or buffer D revealed no difference in the structure of the 3′ half of the *osk3′UTR* RNA under the two salt conditions, indicating that salt does not promote major secondary structure reshaping. We also tested the folding of the presumptive dimerization domain on its own (*oskDD*) (see Fig. 1A), which revealed an enzymatic cleavage profile indistinguishable from that of the full 3′ UTR, indicating that the stem–loop in isolation is robust (data not shown). Thus the predicted structure of the stem–loop is confirmed by the experimental data (Fig. 2A).

To identify the nucleotides that promote RNA dimerization, we compared the RNase T1 cleavage pattern of the *oskDD* RNA under low- and high-salt conditions; this revealed that only guanine 766, located within the palindromic loop, is protected (Fig. 2B, arrow). We also performed dimerization interference experiments, using ethylnitrosourea (ENU), which modifies the phosphates of nucleotides. Sites of modifications on *oskDD* monomers or dimers were identified by alkaline treatment, which induces RNA scission at the modified phosphate. Cleavages present in monomers but absent in dimers indicate the positions at which modification prevents RNA dimerization (negative interference). As shown in Figure 2C, only the modification of nucleotides within the palindromic loop impaired RNA dimerization.

We next determined the dimerization dissociation constant (K_D) of the full-length (data not shown) or the 3′ half of the *osk 3′-UTR* RNAs and of *oskDD* RNA alone (Fig. 2D,E; Supplemental Fig. 1A). In the context of the 3′ half RNA, we also investigated the effect of mutations in the stem–loop on the K_D (Fig. 2D,E). Deletion of the complete stem–loop (*osk3′half-ΔDD*) or of its distal stem (*osk3′half-ΔDDd*) strongly reduced the K_D (Fig. 2D,E). Substitution of four nucleotides in the loop with a GNRA sequence, which disrupts the palindromic sequence while maintaining a loop (Brunel et al. 2002), also resulted in a reduced K_D, indicating that dimerization requires the palindromic sequence of the terminal loop (Fig. 2D,E). We next tested if dimerization indeed occurred in *trans*, by coincubating either complementary or noncomplementary RNA species. While heterodimerization did occur when the complementary RNAs *oskDD* and *osk3′half-WT* (Supplemental Fig. 1B) were coincubated, the K_D was strongly reduced when *oskDD* was coincubated with an RNA bearing a mutation in the palindromic loop sequence (*oskDD* + *osk3′half-GNRA*) (Supplemental Fig. 1C). Finally, substitution of two nucleotides within the palindrome with UU or AA strongly reduced the K_D, whereas dimerization was recovered when the complementary mutant RNAs were coincubated (Fig. 2D). Taken together, we conclude that the *osk* 3′ UTR dimerizes in vitro via a kissing-loop interaction involving six conserved, palindromic nucleotides. We therefore refer to this region as the *osk* mRNA dimerization domain (*oskDD*).

It is interesting to note that *bicoid* RNA oligomerization is initiated by a reversible double loop–loop interaction that is subsequently converted into a stable dimer (Wagner et al. 2004). In contrast, our data support a kissing-loop model for *osk* RNA dimerization that is highly similar to that proposed for dimerization of retroviral RNAs. Indeed, dimerization of both *osk* and *HIV-1* RNAs is initiated by a 6-nt, GC-rich palindrome (Clever et al. 1996).

oskar dimerization loop base-pairing promotes coassembly of RNA molecules in vivo

To test if the dimerization domain might contribute to the hitchhiking of *osk* 3′-UTR-containing reporters with endogenous *osk* mRNA in vivo (Hachet and Ephrussi 2004), we fused *egfp* to the *osk* 3′ UTRs tested for dimerization in vitro (Fig. 1A) and assayed the distribution of *egfp* RNA in the oocyte, comparing it with that of endogenous *osk* (see

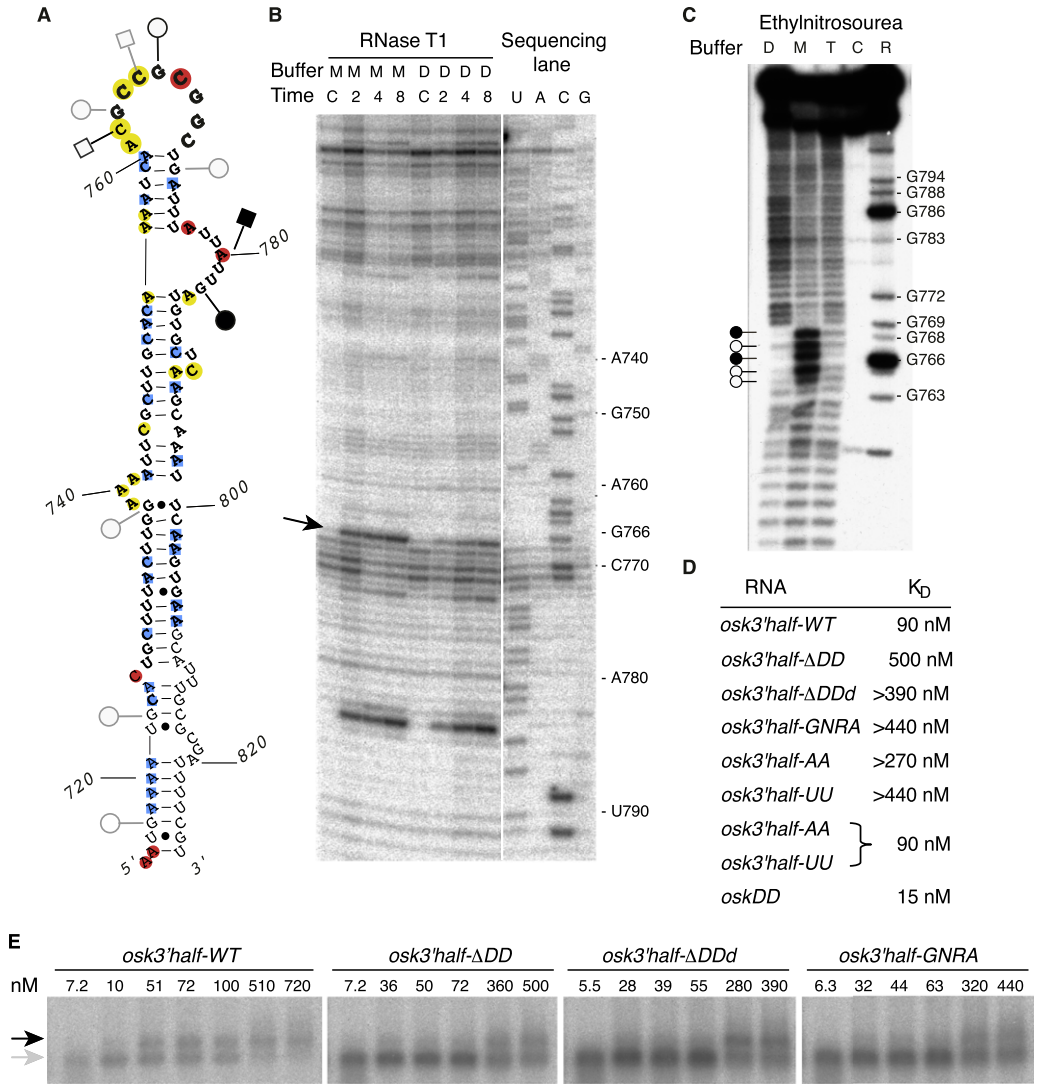

FIGURE 2. A secondary structure in the 3′ half of the *osk* 3′ UTR promotes dimerization. (*A*) Proposed secondary structure of nucleotides 714–827, the conserved region within the dimerization-competent portion of the *osk* 3′ UTR. Data supporting this prediction were collected by chemical (dimethyl-sulfate, DMS) and enzymatic (RNase T1 and T2) probing and are summarized in the figure. DMS (blue squares, weak; yellow circles, medium; red circles, strong modification) modifies unpaired adenines and cytosines, RNase T1 (solid circle, strong; open circle, medium; gray open circle, weak cleavage) cleaves unpaired guanines, and RNase T2 (solid square, strong; open square, medium; gray open square, weak cleavage) efficiently targets single-stranded nucleotides with a preference for adenines. (*B*) Enzymatic probing of the 3′ half of the *osk* 3′ UTR using RNase T1. Hydrolysis was conducted in buffer M or D, and the reaction was incubated for 2, 4, and 8 min. An incubation control (C) was included that did not contain the enzyme. Sequencing lanes (*U*,*A*,*C*,*G*) were run in parallel. Nucleotide 766 was specifically protected in buffer D but not in buffer M (arrow). (*C*) Phosphate ethylation interference by ENU. Autoradiography of the fractionation gel after modification conducted on the dimerization domain of *osk* RNA. (M and D) RNA extracted from the monomer and the dimer bands, respectively; (T) total population of modified RNA; (C) incubation control. Lane *R* corresponds to the RNase T1 ladder. Negative interference is indicated by circles: A complete disappearance of a band revealed a "strong" interference (solid circle), a slight disappearance of a band indicated a "weak" interference (open circle). (*D*) Summary of experiments probing the dimerization capacity (K_D) of *osk3′*half wild-type, *osk* 3′half RNAs with mutations in the conserved stem–loop region and *oskDD*. Association of RNAs was strongly reduced when RNAs with partial or complete deletion of the stem–loop (*osk3′half-ΔDD*, *-ΔDDd*) or with substitutions in the terminal loop were analyzed. Dimerization was restored when RNAs with compensatory mutations (*osk3′half-AA* and *-UU*) were coincubated. K_D's are indicated on the *right*. (*E*) Kinetics of dimerization of *osk3′half-WT*, *osk3′half-ΔDD*, *osk3′half-ΔDDd*, and *osk3′half*-GNRA RNAs as a function of RNA concentration. Indicated is the amount of nonradioactive RNA (nanomolar, nM); in addition, trace amounts of radioactive RNAs were added for visualization. Representative autoradiographs of the agarose gels show monomeric (gray arrow) and dimeric (black arrow) RNA species. Fifty percent of *osk3′half-WT* RNA formed dimers at 72–100 nM. RNAs bearing a mutation in the dimerization domain dimerized at >400 nM.

below). The chimeric *egfp* transgenes, which contained no introns, were expressed under the control of the *maternal tubulin* promoter using the UAS-Gal4 system (Fig. 3A). The wild-type (*egfp-WT*) and mutant (*egfp-UU* and *egfp-GNRA*) RNAs were expressed at similar levels as judged by qRT-PCR analysis on whole ovaries (Fig. 3A′).

Transport of *osk* mRNA from the nurse cells into the oocyte during early oogenesis is mediated by the 3′ UTR (Jenny et al. 2006). Confirming that the *osk* 3′ UTR is sufficient, and that hitchhiking is not required for this first step in transport, the *egfp* reporter RNAs were enriched in the oocyte at stage 6 (Fig. 3B,G,L). During mid-oogenesis, *osk* mRNA is transported within the oocyte to the posterior pole, and it is for this second step in localization that hitchhiking becomes critical (Hachet and Ephrussi 2004). Our analysis of the *egfp* reporter RNAs at stage 9 showed that mutation of the dimerization domain selectively affected the ability of the mutant reporters to localize at the posterior pole (Fig. 3C,H,M, quantification in Fig. 3Q). Localization of endogenous *osk* mRNA was unaffected by the presence of the reporter RNAs (Fig. 3E,J,O), and in all cases, Osk protein was detected at the posterior pole, confirming that endogenous *osk* RNA was correctly localized and translated (Fig. 3F,K,P). The *osk* mRNA and Osk protein levels in the transgenic lines are, in fact, highly similar to those in the w^{1118} control (Fig. 3R,S).

Both wild-type and mutant reporter RNAs could be detected at the posterior at stage 10 (Fig. 3D,I,N), when cytoplasmic streaming and Osk protein-dependent trapping result in posterior accumulation of *osk* 3′-UTR-containing RNAs (Glotzer et al. 1997). The reduced posterior enrichment of the mutated *egfp* reporter RNAs at stage 9 clearly indicates that the dimerization domain promotes the *osk* 3′-UTR-dependent hitchhiking of RNA molecules in vivo.

To test if *osk* hitchhiking involves direct base-pairing, we first generated the *oskAA* transgene, which bears a 2-nt AA substitution (Fig. 1A) in the dimerization loop of an otherwise wild-type, intron-containing, *osk* gene (*oskWT*) (Hachet and Ephrussi 2004). The *oskWT* and *oskAA* transgenes were crossed into the *osk* RNA null background, such that in each case the transgene was the only source of *osk* RNA in the oocyte (thereafter referred to as *oskWT* or *oskAA* oocytes). *oskAA* rescued the developmental arrest at stage 7 of oogenesis that is the primary defect in egg chambers completely null for *osk* mRNA (Jenny et al. 2006). In situ hybridization confirmed that, just like *oskWT* RNA, *oskAA* RNA was enriched in and localized at the posterior pole in the majority of *osk* RNA null mutant oocytes (Fig. 4A,A′,B,B′). Therefore, the presence of a palindromic sequence in the dimerization loop is not essential for posterior localization of full-length, spliced *osk* RNA molecules, which can localize on their own (Hachet and Ephrussi 2004).

Our in vitro analysis showed that *osk* RNA dimerizes through kissing-loop interactions (Fig. 2E). We therefore assessed the ability of *oskAA* RNA to associate in vivo with the complementary *egfp-UU* RNA and promote its localization at the posterior pole. Simultaneous expression of the *egfp-UU* and *oskAA* transgenes in the *osk* RNA null background resulted in posterior localization of *egfp-UU* RNA in the majority of oocytes (Fig. 4D′). In contrast, coexpression of the *egfp-WT* reporter with *oskAA* led to a posterior enrichment of the noncomplementary *egfp-WT* RNA in only a minority of oocytes (Fig. 4C′). In both cases, the presence of Staufen protein at the posterior pole confirmed that *oskAA* RNA was correctly localized (Fig. 4C,D), and in situ hybridization confirmed that *egfp* RNAs were correctly enriched in stage 6 oocytes (Fig. 4C,D).

We therefore conclude that base-pairing interactions between the dimerization loops of unspliced reporter RNA and spliced, localization-competent *osk* RNA molecules occur in vivo.

CONCLUDING REMARKS

In this study, we have shown that the dimerization domain mediates hitchhiking of *osk* 3′-UTR-containing reporter RNAs. In the future, it will be interesting to determine the in vivo role of this domain and of hitchhiking in the regulation endogenous *osk* mRNA. It is likely that dimerization is involved in other aspects of *osk* regulation. Interestingly,

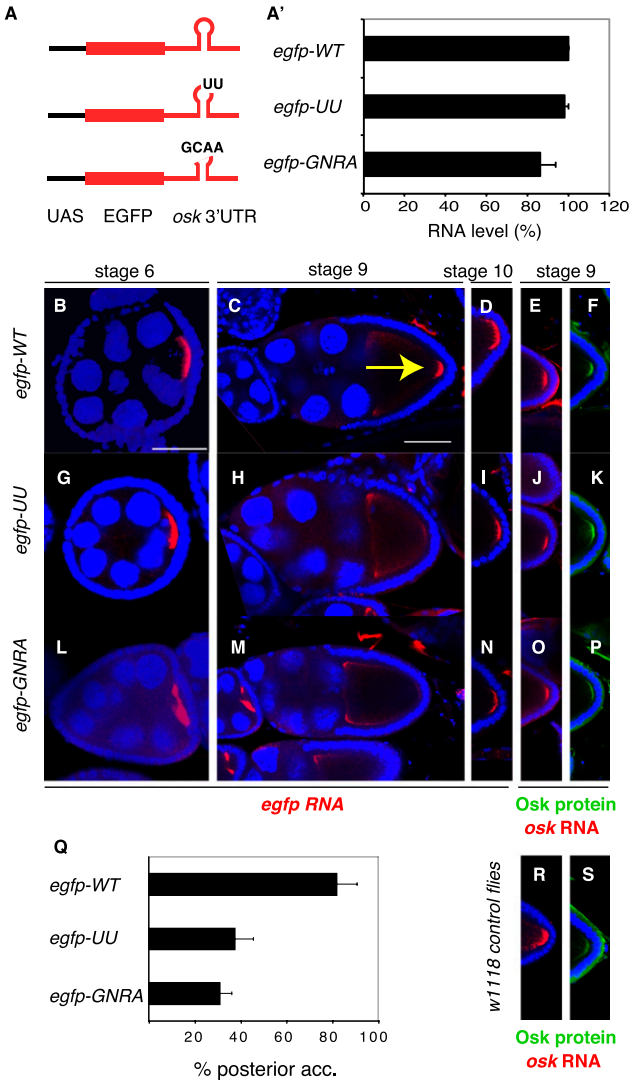

FIGURE 3. (Legend on next page)

Reveal et al. (2010) recently proposed that translational activation of *osk* molecules can occur in *trans*, which could also involve RNA dimerization.

The palindromic sequence that initiates oligomerization of *osk* mRNAs is not present in other transcripts enriched at the posterior pole such as *nanos* and *cyclinB* (data not shown). However, other RNAs have been shown to undergo dimerization. In the case of *bicoid* mRNA, in vitro dimerization requires a single stem–loop (but is not initiated by a palindromic loop), whereas particle formation upon *bicoid* RNA injection into living embryos also requires other parts of the 3′ UTR (Wagner et al. 2001). The *HIV-1* dimerization initiation site (*DIS*) promotes RNA dimerization in vitro, while formation of a stable duplex requires proteins to consolidate the initial kissing-loop interaction (Russell et al. 2004; Lever 2007). In the case of *osk* mRNA, both Bruno and PTB proteins have been shown to promote *osk* 3′ UTR RNA oligomerization (Chekulaeva et al. 2006; Besse et al. 2009). In view of the multiple means through which *osk* RNA molecules can interact and oligomerize, it is remarkable that the RNA–RNA interaction detected in vitro has a discernable effect on hitchhiking in vivo. The redundancy of mechanisms mediating the association of *osk* RNA molecules can explain the apparently normal localization of *oskAA* RNA at the posterior pole. Whereas a kissing-loop interaction via the dimerization domain may nucleate the formation of *osk* RNA dimers, their stabilization and assembly into higher-order structures, similar to *HIV* dimerization, most likely involves additional elements in the 3′ UTR.

The phenomenon of RNA hitchhiking was revealed by the observation that both unspliced *osk* mRNA and reporter RNAs bearing the *osk* 3′ UTR fail to localize in oocytes lacking endogenous, localization-competent *osk* mRNA. The significance of splicing for *osk* mRNA localization is thought to reside, at least in part, in the involvement of the exon-junction complex of proteins, whose association with mRNAs is splicing-dependent (Hachet and Ephrussi 2004 and references therein). Hitchhiking via RNA–RNA dimerization, consolidated by protein association, could provide a versatile and powerful means for a given mRNA to achieve different localizations within different cellular contexts. It is becoming increasingly apparent that many of the RNA-binding proteins and the machineries that mediate mRNA transport are highly conserved and expressed in numerous cell types. Thus, mRNAs encoding localization signals often display a similar localization pattern in different types of cells (Kislauskis et al. 1993; Bassell et al. 1998). In contrast, a hitchhiking mRNA could be independently targeted to distinct locations by its association with localization-competent "driver" mRNAs destined for distinct intracellular locations. Thus, the final localization of hitchhiking mRNAs would depend on the mRNA landscape of the cell in which it is expressed. It will be of great interest to determine the extent to which hitchhiking underlies the intracellular localization of mRNAs in eukaryotic cells and to identify the codes that mediate the association of localization-incompetent mRNAs with their localization-competent mRNA partners.

FIGURE 3. The dimerization domain promotes *osk* RNA interaction during hitchhiking in vivo. (*A*) Schematic representation of the reporter constructs used in this panel. (*A′–Q*). Egg chambers from w^{1118} flies expressing *egfp-WT*, *-UU*, or *-GNRA* under the control of a *mat-α4-tub*-Gal4 driver. (*A′*) qRT-PCR experiment probing the relative levels of gene expression of *egfp-WT*, *egfp-UU*, and *egfp-GNRA* RNAs. RNA expression is shown as the percentage of the *egfp-WT* RNA level. All RNA levels were normalized to *rp49* RNA. (*B–P,R,S*) Reporter RNAs are detected using an *egfp*-antisense probe, endogenous *osk* is visualized using a probe antisense to the *osk* coding sequence, and Osk protein is stained with anti-Osk antibodies. All egg chambers shown were counterstained with DAPI (blue). Bar, 50 μm. The panels highlighting the posterior pole of different oocytes (*D–F,I–K,N–P*) show images at the same magnification as *C*, *H*, and *M*. (*B,G,L*) *egfp-WT*, *-UU*, and *GNRA* reporter RNAs accumulate in young oocytes (stage 6). (*C,H,M*) Posterior accumulation of mutant *egfp-UU* and *-GNRA* reporter RNAs is strongly reduced in comparison with *egfp-WT* RNA at stage 9. The arrow in *C* indicates the position of the posterior pole. (*D,I,N*) *egfp-WT*, and to a lesser degree also *egfp-UU* and *-GNRA*, RNAs are present at the posterior pole of stage 10 oocytes. (*E,J,O*) Endogenous *osk* mRNA at stage 9 is localized in the presence of reporter RNAs. (*F,K,P*) Osk protein is expressed in stage 9 oocytes in the presence of reporter RNAs. (*Q*) Percentage of oocytes showing a posterior accumulation of *egfp-WT*, *-UU*, or *-GNRA* reporter RNAs in stage 9 egg chambers. The accumulation of *egfp* RNAs was scored in at least two independent experiments (*egfp-WT*: $n = 127$; *egfp-UU*: $n = 61$; *egfp-GNRA*: $n = 71$). (*R,S*) w^{1118} control flies, which do not express transgenic *reporter3′UTR*, were also stained for *osk* mRNA and Osk protein for comparison.

MATERIALS AND METHODS

Plasmids

osk *3′ UTR*

A StyI–MaeIII fragment of the plasmid pBS-*osk* 3′ UTR was subcloned into the StuI site of the pUT7 vector, a pUC18 derivative containing a T7 RNA polymerase. *osk5′half* (nucleotides 1–616) and *osk3′-half* (nucleotides 616–1151) of *osk* 3′ UTR were cloned into the StuI site of the pUT7 vector. *oskDD* (the dimerization domain, nucleotides 714–827) was PCR-amplified from the *osk* 3′-UTR DNA. *osk 3′UTR-ΔDD*, *-ΔDDd*, *-GNRA*, *-AA*, and *-UU* were generated by PCR mutagenesis (Quick Change PCR kit; QIAGEN). The complete dimerization domain is deleted in *osk 3′UTR-ΔDD* (nucleotides 715–827), while only the distal stem is deleted in *osk 3′UTR-ΔDDd* (nucleotides 736–802). In *osk 3′UTR-AA*, *-UU*, and *-GNRA*, nucleotides of the terminal loop are substituted (*AA*, nucleotides 768–769; *UU*, nucleotides 764–765; *GNRA*, nucleotides 765–768).

osk *3′-UTR orthologs from* D. yakuba, D. pseudoobscura, D. immigrans, D. mercantorum, *and* Z. sepsoides

Total ovary RNA was isolated (TRIzol; Invitrogen), poly(A) RNAs were enriched (mRNA Purification Kit; DynaBeads), and cDNAs were generated (Superscript First Strand Synthesis; Invitrogen). Sequences were amplified with a specific primer against the *osk* coding region and an oligo(TT) primer. PCR products were TA-cloned and sequenced. Sequences were aligned (ClustalW), and the secondary structures were predicted with mfold v2.3 at 25°C (Zuker 2003).

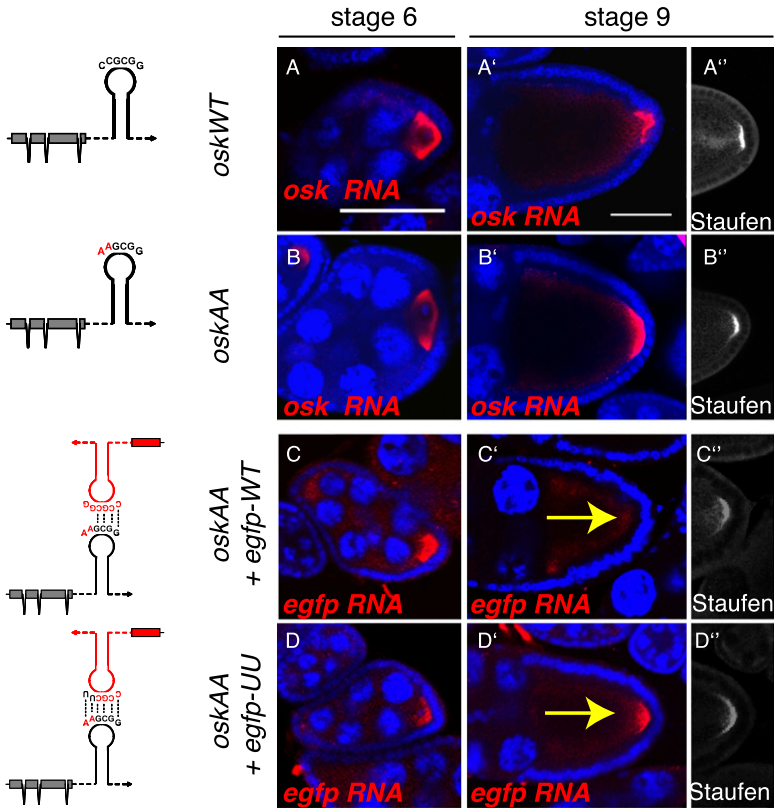

FIGURE 4. *osk* RNAs engage in direct interactions in the oocyte. Egg chambers from *osk* RNA null flies [;;osk^{A87}/Df(3R)p^{XT103}] expressing full-length transgenic *osk* mRNA under the control of *pCog* and *nos*-Gal4 drivers. (*A–A″*,*B–B″*) RNA expressed from *oskWT* (*A–A″*) and *oskAA* (*B–B″*) transgenes is transported into the oocyte (stage 6) and localizes at the posterior pole of stage 9 egg chambers (*oskWT*, 93%; *oskAA*, 91%). In a subset of the egg chambers (*oskWT*, 30%; *oskAA*, 39%), ectopic *osk* mRNA is additionally detected. Staufen protein is equally enriched at the posterior pole of egg chambers. As established by qRT-PCR, *oskWT* and *oskAA* were overexpressed to similar levels in comparison to *osk* levels of w^{1118} flies. *osk* RNAs were detected using an *osk* (coding region)–antisense probe (red) immuno-stained with anti-Staufen antibodies (white). (*C–C″*,*D–D″*) Egg chambers coexpressing *oskAA* with either *egfp-WT* or *egfp-UU*. Both reporter RNAs enrich in young oocytes (*C*,*D*), but posterior pole accumulation of the *egfp-WT* is strongly reduced (*C′*) (16% ± 13%) compared with the *egfp-UU* (*D′*) (91% ± 5%) at stage 9 of oogenesis. Staufen enriches equally in the presence of either RNA (*C″*,*D″*). A summary of *reporter3′UTR* RNA hitchhiking at stage 9 of oogenesis is shown *below*. All egg chambers were simultaneously stained with *egfp*-antisense probe (red) to specifically detect the reporter RNAs and anti-Staufen antibodies (white) to also detect full-length *osk* mRNA. The accumulation of *egfp*-reporter RNA at the posterior pole was scored in at least two independent experiments, analyzing at least 15 egg chambers per experiment. All egg chambers were stained for RNA (red) by whole-mount in situ hybridization and counterstained with DAPI (blue). Bar, 50 μm.

The genes of interest (*osk3′UTR-WT*, *-GNRA*, *-UU*, and *-region2*, *D. pseudooscura* and *D. virilis osk* 3′ UTRs) were PCR-amplified from pUT7 templates with primers attaching BamHI restriction sites, and TA-cloned. BamHI fragments were then subcloned into pUASpGWΔK10 to generate the respective *egfp* RNAs. To generate pUASpGWΔK10, the K10 terminator was removed from pUASp (Rorth 1998) by XbaI and PstI digestion, blunting, and religation of pUASp. The *egfp* open reading frame (ORF) was amplified from pCRII-TOPO-EGFP with primers attaching KpnI and NotI sites, digested, and cloned to KpnI NotI-digested pUASpΔK10.

oskWT was previously described (Hachet and Ephrussi 2004). To generate *oskAA*, an AfeI–BstZ171 fragment of pSP72-*oskWT* was replaced with the respective fragment from pUC18T7-*osk* 3′UTR-AA. *oskAA* was then PCR-amplified attaching BamHI restriction sites and ligated to BamHI-digested pUASpΔK10. Primer sequences are available upon request.

RNA synthesis and in vitro dimerization

In vitro transcription was conducted as previously described (Wagner et al. 2001, 2004) using BamHI-linearized plasmid DNA as template. RNA dimerization was performed as previously described (Wagner et al. 2001). Dimerization buffer D contained 50 mM sodium cacodylate (pH 7.5), 300 mM KCl, and 5 mM $MgCl_2$, while monomers were obtained in buffer M (50 mM sodium cacodylate at pH 7.5, 50 mM KCl, 0.1 mM $MgCl_2$). Large RNA fragments were analyzed as described (Wagner et al. 2001), while short RNA fragments were resolved at 4°C by electrophoresis using 12% acrylamide/(bis-acrylamide 1/30) gels.

K_d determination

The apparent dissociation constant (K_D) of the dimer was determined by mixing increasing concentration of unlabeled RNA (between 4.6 nM and 300 nM) with a negligible constant concentration of labeled RNA (<1 nM) (Wagner et al. 2004). Dimerization was conducted under standard dimerization conditions (see above). The concentration of unlabeled RNA in the experiments ranged from 0.15 to 720 nM. All experiments were performed at least twice.

Probing and footprinting experiments

RNA probing was carried out as previously described (Wagner et al. 2004). *osk* RNA (750 ng), in the presence of tRNA (1.5 μg), was incubated in buffers allowing or prohibiting dimerization, respectively, before subjecting it to RNase hydrolysis or chemical modification. Typically, incubation in buffer D yielded 50% of dimeric and 50% of monomeric RNA, while 100% monomers were formed in buffer M. Enzymatic hydrolysis was performed with 0.2 units of RNase T1 (Pharmacia), 0.1 unit of RNase T2 (Sigma), and 0.1 unit of RNase V1 (Pharmacia). Dimethylsulfate (DMS; Aldrich) reaction was allowed to proceed for 2, 4, or 8 min. Modifications were detected using 10% polyacrylamide/8 M urea gel.

Phosphate modification interference

The appropriate 5′-end-labeled fragment of the *osk* dimerization domain (10 ng) was alkylated on its phosphate groups by ethylnitrosourea (ENU) essentially as described before (Wagner et al.

2004). Modifications were allowed for 1 min at 90°C with 0.32 volume of ENU-saturated ethanol in 25 μL of 50 mM sodium cacodylate (pH 6.5), 50 mM KCl, and 1 mM EDTA, in the presence of 1 μg of total tRNA. End-labeled RNA fragments were separated on a 12% polyacrylamide/8 M urea gel. To control RNA modification, the end-labeled RNA was submitted to the phosphate modification procedure using the same modification conditions, then directly submitted to the ethylated phosphate cleavage procedure without purification of the monomeric and dimeric species. Experiments were conducted twice.

qRT-PCR

Quantitative RT-PCR was performed on cDNAs generated from ovaries of flies expressing the respective transgenes. Amplified product was detected using the SYBRGreen (Ambion) system on an ABIPrism7500 real-time PCR apparatus. The *egfp* portion of the transgenic RNAs was amplified using primers specific for the EGFP ORF and normalized to *rp49*. The amplification efficiency was determined using serial dilutions of a cDNA mix from all samples.

Assaying *osk* RNA hitchhiking in egg chambers

Transgenes were expressed in the germline using the *maternal-α-tubulin*-Gal4 driver. For expression of *oskAA* and coexpression of *oskAA* with *egfp*-reporter variants in *osk* RNA null flies, the *pCog* and *nanos* Gal4 drivers were combined. Lines with equivalent mRNA expression levels, as judged by in situ hybridization and qRT-PCR, were used. To score hitchhiking, posterior enrichment of the *egfp* reporter RNAs in the oocyte at stage 9 was measured. In each experiment, posterior enrichment was monitored in at least 20 egg chambers. Only egg chambers with posterior Staufen protein, indicative of posterior *osk* mRNA localization, were scored. At least two individual transgenic insertion lines were analyzed in parallel, and experiments were repeated at least three times.

Whole-mount in situ hybridization

In situ hybridization was performed as described (Hachet and Ephrussi 2004). Antisense probes for the *egfp* and *osk* coding sequences (cds) were generated by in vitro transcription (Ambion; Megascript) and detected using HRP-conjugated sheep anti-DIG antibody (1:200; Roche) followed by Cy3-tyramide signal amplification (Perkin Elmer).

Whole-mount immuno/in situ hybridization

Immunostaining coupled with in situ hybridization was carried out as previously described (Vanzo and Ephrussi 2002), and antigens were detected using rabbit anti-Staufen (1:1500) and rat anti-Osk (1:3000) antibodies. Cy5 (Jackson Immuno Research Laboratories) and AlexaFluor488 (Invitrogen) coupled secondary antibodies were used at 1:500 dilution.

Fly stocks

The following wild-type flies were used: w^{1118} (wild-type control); *D. yakuba* and *D. pseudoobscura* (a gift from M. Ashburner); and *D. immigrans*, *D. mercantorum*, and *Z. sepsoides* (a gift from R. Lehmann). The following mutant fly stocks were used: osk^{A87} (Vanzo and Ephrussi 2002) and $Df(3R)p^{XT103}$ (Lehmann and Nusslein-Volhard 1986), which in combination are null for *osk* RNA (Jenny et al. 2006). UAS-coupled genes were expressed in the germline using *pCog-Gal4:VP16* (Rorth 1998), *nanos-Gal4:VP16* (Rorth 1998), and *mat-α4-tub-Gal4:VP16* (Bloomington stock #7062) promoters.

Microscope

For all analyses, a confocal microscope (DMR-E; Leica) equipped with a scan head (TCS SP2 AOBS; Leica) and an oil-immersion 20×, 1.4 NA objective was used. Images were acquired at a 2× zoom and edited with Adobe Photoshop CS.

SUPPLEMENTAL MATERIAL

Supplemental material is available for this article.

ACKNOWLEDGMENTS

We are grateful to Sandra Müller and Ann-Mari Voie for *Drosophila* transgenesis. We thank Ruth Lehmann and Michael Ashburner for fly stocks, Laurence Ettwiller for assistance with multiple sequence alignments, and Katherine Brown for critical reading of the manuscript. We are especially indebted to Virginie Marchand for critical discussion of the manuscript and data. H.J. was supported in part by a fellowship of the Christiane Nüsslein-Volhard Foundation.

Received February 22, 2011; accepted August 23, 2011.

REFERENCES

Bassell GJ, Zhang H, Byrd AL, Femino AM, Singer RH, Taneja KL, Lifshitz LM, Herman IM, Kosik KS. 1998. Sorting of β-actin mRNA and protein to neurites and growth cones in culture. *J Neurosci* **18:** 251–265.

Besse F, López de Quinto S, Marchand V, Trucco A, Ephrussi A. 2009. *Drosophila* PTB promotes formation of high-order RNP particles and represses *oskar* translation. *Genes Dev* **23:** 195–207.

Brunel C, Marquet R, Romby P, Ehresmann C. 2002. RNA loop–loop interactions as dynamic functional motifs. *Biochimie* **84:** 925–944.

Chekulaeva M, Hentze MW, Ephrussi A. 2006. Bruno acts as a dual repressor of *oskar* translation, promoting mRNA oligomerization and formation of silencing particles. *Cell* **124:** 521–533.

Clever JL, Wong ML, Parslow TG. 1996. Requirements for kissing-loop-mediated dimerization of human immunodeficiency virus RNA. *J Virol* **70:** 5902–5908.

Ephrussi A, Lehmann R. 1992. Induction of germ cell formation by *oskar*. *Nature* **358:** 387–392.

Ephrussi A, Dickinson LK, Lehmann R. 1991. *oskar* organizes the germ plasm and directs localization of the posterior determinant *nanos*. *Cell* **66:** 37–50.

Ferrandon D, Koch I, Westhof E, Nüsslein-Volhard C. 1997. RNA–RNA interaction is required for the formation of specific *bicoid* mRNA 3′ UTR–STAUFEN ribonucleoprotein particles. *EMBO J* **16:** 1751–1758.

Fu W, Gorelick RJ, Rein A. 1994. Characterization of human immunodeficiency virus type 1 dimeric RNA from wild-type and protease-defective virions. *J Virol* **68:** 5013–5018.

Glotzer JB, Saffrich R, Glotzer M, Ephrussi A. 1997. Cytoplasmic flows localize injected *oskar* RNA in *Drosophila* oocytes. *Curr Biol* **7:** 326–337.

Hachet O, Ephrussi A. 2004. Splicing of *oskar* RNA in the nucleus is coupled to its cytoplasmic localization. *Nature* **428:** 959–963.

Jenny A, Hachet O, Zavorszky P, Cyrklaff A, Weston MD, Johnston DS, Erdelyi M, Ephrussi A. 2006. A translation-independent role of *oskar* RNA in early *Drosophila* oogenesis. *Development* **133:** 2827–2833.

Kim-Ha J, Smith JL, Macdonald PM. 1991. *oskar* mRNA is localized to the posterior pole of the *Drosophila* oocyte. *Cell* **66:** 23–35.

Kim-Ha J, Webster PJ, Smith JL, Macdonald PM. 1993. Multiple RNA regulatory elements mediate distinct steps in localization of *oskar* mRNA. *Development* **119:** 169–178.

Kim-Ha J, Kerr K, Macdonald PM. 1995. Translational regulation of *oskar* mRNA by Bruno, an ovarian RNA-binding protein, is essential. *Cell* **81:** 403–412.

Kislauskis EH, Li Z, Singer RH, Taneja KL. 1993. Isoform-specific 3′-untranslated sequences sort α-cardiac and β-cytoplasmic actin messenger RNAs to different cytoplasmic compartments. *J Cell Biol* **123:** 165–172.

Kung HJ, Bailey JM, Davidson N, Nicolson MO, McAllister RM. 1975. Structure, subunit composition, and molecular weight of RD-114 RNA. *J Virol* **16:** 397–411.

Lehmann R, Nusslein-Volhard C. 1986. Abdominal segmentation, pole cell formation, and embryonic polarity require the localized activity of *oskar*, a maternal gene in *Drosophila*. *Cell* **47:** 141–152.

Lever AML. 2007. HIV-1 RNA packaging. *Adv Pharmacol* **55:** 1–32.

Marquet R, Baudin F, Gabus C, Darlix JL, Mougel M, Ehresmann C, Ehresmann B. 1991. Dimerization of human immunodeficiency virus (type 1) RNA: stimulation by cations and possible mechanism. *Nucleic Acids Res* **19:** 2349–2357.

Martin KC, Ephrussi A. 2009. mRNA localization: Gene expression in the spatial dimension. *Cell* **136:** 719–730.

Reveal B, Yan N, Snee MJ, Pai CI, Gim Y, Macdonald PM. 2010. BREs mediate both repression and activation of *oskar* mRNA translation and act in *trans*. *Dev Cell* **18:** 496–502.

Rorth P. 1998. Gal4 in the *Drosophila* female germline. *Mech Dev* **78:** 113–118.

Russell RS, Liang C, Wainberg MA. 2004. Is HIV-1 RNA dimerization a prerequisite for packaging? Yes, no, probably? *Retrovirology* **1:** 23. doi: 10.1186/1742-4690-1-23.

Smith JL, Wilson JE, Macdonald PM. 1992. Overexpression of *oskar* directs ectopic activation of *nanos* and presumptive pole cell formation in *Drosophila* embryos. *Cell* **70:** 849–859.

Vanzo NF, Ephrussi A. 2002. Oskar anchoring restricts pole plasm formation to the posterior of the *Drosophila* oocyte. *Development* **129:** 3705–3714.

Wagner C, Palacios I, Jaeger L, St Johnston D, Ehresmann B, Ehresmann C, Brunel C. 2001. Dimerization of the 3′UTR of *bicoid* mRNA involves a two-step mechanism. *J Mol Biol* **313:** 511–524.

Wagner C, Ehresmann C, Ehresmann B, Brunel C. 2004. Mechanism of dimerization of bicoid mRNA: Initiation and stabilization. *J Biol Chem* **279:** 4560–4569.

Webster PJ, Suen J, Macdonald PM. 1994. *Drosophila virilis oskar* transgenes direct body patterning but not pole cell formation or maintenance of mRNA localization in *D. melanogaster*. *Development* **120:** 2027–2037.

Wilhelm JE, Hilton M, Amos Q, Henzel WJ. 2003. Cup is an eIF4E binding protein required for both the translational repression of *oskar* and the recruitment of Barentsz. *J Cell Biol* **163:** 1197–1204.

Zuker M. 2003. Mfold web server for nucleic acid folding and hybridization prediction. *Nucleic Acids Res* **31:** 3406–3415.

Dimerization of *oskar* 3′ UTRs promotes hitchhiking for RNA localization in the *Drosophila* oocyte

Helena Jambor, Christine Brunel and Anne Ephrussi

RNA 2011 17: 2049-2057 originally published online October 25, 2011
Access the most recent version at doi:10.1261/rna.2686411